

## Structures and Ligand Exchange of N-Confused Porphyrin Dimer Complexes with Group 12 Metals

Hiroyuki Furuta,<sup>\*,†,‡</sup> Tatsuki Morimoto,<sup>†,§</sup> and Atsuhiko Osuka<sup>§</sup>

Department of Chemistry and Biochemistry, Graduate School of Engineering, Kyushu University, Fukuoka 812-8581, Japan, and PRESTO, JST, and Department of Chemistry, Graduate School of Science, Kyoto University, Kyoto 606-8502, Japan

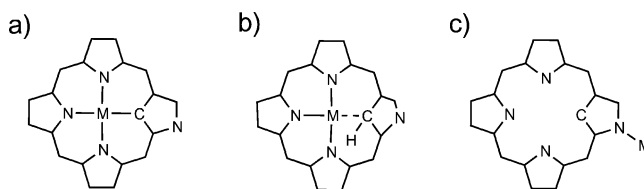
Received November 9, 2003

N-confused 5,20-diphenylporphyrin (NCDPP, **1**) formed 2:2 dimer complexes with group 12 metals both in the solid state and in solution. X-ray single-crystal analyses of the Zn(II) and Cd(II) complexes (**7**, **8**) revealed that each metal ion is coordinated with three inner core nitrogens and a peripheral nitrogen of the other NCDPP in the pair. In the <sup>1</sup>H NMR spectra of **7**, **8**, and the Hg(II) complex (**9**), the outer α-H signals of the *confused* pyrrole ring appeared in the upfield region at 2.57, 3.44, and 3.60 ppm, respectively, due to the ring current effect by the coordinated porphyrins. In the case of the Cd(II) and Hg(II) complexes (**8**, **9**), additional magnetic couplings with the metal nuclei of the partner rings were observed. The equilibrium constants (*K*) of the monomer exchange reaction at 25 °C were determined to be 2.5, 1.3, and 0.6 for the (Zn–Cd), (Cd–Hg), and (Zn–Hg) heterodimer complexes, respectively, from the <sup>1</sup>H NMR spectra of a solution containing two different dimers. Furthermore, a metal-transfer reaction from a Zn(II) NCP dimer complex to the free base porphyrin was demonstrated.

## Introduction

Metalloporphyrins bearing an additional binding center at the periphery are attracting considerable attention as useful building blocks for the multiporphyrin assemblies.<sup>1</sup> Among such porphyrins, N-confused porphyrin (NCP),<sup>2</sup> an isomer of porphyrin, is of particular interest because it possesses two metal binding sites already in the framework, namely, the inner N<sub>3</sub>C core and the peripheral N of the *confused* pyrrole ring. Hitherto, NCP has been shown to coordinate metals in the core forming neutral square-planar complexes possessing a carbon–metal bond (Chart 1a) for Ni(II),<sup>2b</sup> Cu-

Chart 1. Schematic Drawings of the Typical Coordination Modes of NCP: (a) Square Planar; (b) Side-On η<sup>1</sup>-Interaction; (c) Outer-N Coordination



(II),<sup>3a,b</sup> Cu(III),<sup>3c</sup> Pd(II),<sup>3d</sup> Pt(II),<sup>3e</sup> Mn(III),<sup>3f</sup> Ag(III),<sup>3g</sup> a hexacoordinated complex with Sb(V),<sup>3h</sup> and side-on η<sup>1</sup>-coordination type complexes with Zn(II),<sup>4a</sup> Mn(II),<sup>3f,4b</sup> and Fe(II)<sup>4c</sup> (Chart 1b). On the other hand, outer-N coordinated

\* To whom correspondence should be addressed. E-mail: hfuruta@csf.kyushu-u.ac.jp.

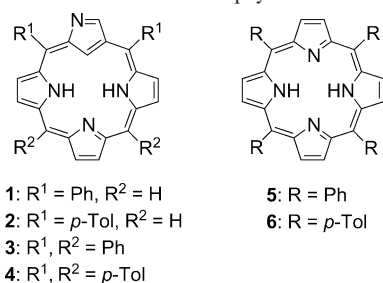
† Kyushu University.

‡ PRESTO, JST.

§ Kyoto University.

- (1) (a) Wojaczyński, J.; Latos-Grażyński, L. *Coord. Chem. Rev.* **2000**, *204*, 113–171. (b) Richeter, S.; Jeandon, C.; Gisselbrecht, J.-P.; Ruppert, R.; Callot, H. J. *J. Am. Chem. Soc.* **2002**, *124*, 6168–6179. (c) Michelsen, U.; Hunter, C. A. *Angew. Chem., Int. Ed.* **2000**, *39*, 764–767. (d) Takahashi, Y.; Kobuke, Y. *J. Am. Chem. Soc.* **2003**, *125*, 2372–2373. (e) Imamura, T.; Funatsu, K.; Ye, S.; Morioka, Y.; Uosaki, K.; Sasaki, Y. *J. Am. Chem. Soc.* **2000**, *122*, 9032–9033. (2) (a) Furuta, H.; Asano, T.; Ogawa, T. *J. Am. Chem. Soc.* **1994**, *116*, 767–768. (b) Chmielewski, P. J.; Latos-Grażyński, L.; Rachlewicz, K.; Głowiak, T. *Angew. Chem., Int. Ed. Engl.* **1994**, *33*, 779–781. (c) Latos-Grażyński, L. In *The Porphyrin Handbook*; Kadish, K. M., Smith, K. M., Guillard, R., Eds.; Academic Press: San Diego, CA, 2000; Vol. 2, Chapter 14. (d) Furuta, H.; Maeda, H.; Osuka, A. *Chem. Commun.* **2002**, 1795–1804.

- (3) (a) Chmielewski, P. J.; Latos-Grażyński, L.; Schmidt, I. *Inorg. Chem.* **2000**, *39*, 5475–5482. (b) Maeda, H.; Osuka, A.; Ishikawa, Y.; Aritome, I.; Hisaeda, Y.; Furuta, H. *Org. Lett.* **2003**, *5*, 1293–1296. (c) Maeda, H.; Ishikawa, Y.; Matsuda, T.; Osuka, A.; Furuta, H. *J. Am. Chem. Soc.* **2003**, *125*, 11822–11823. (d) Furuta, H.; Kubo, N.; Maeda, H.; Ishizuka, T.; Osuka, A.; Nanami, H.; Ogawa, T. *Inorg. Chem.* **2000**, *39*, 5424–5425. (e) Furuta, H.; Youfu, K.; Maeda, H.; Osuka, A. *Angew. Chem., Int. Ed.* **2003**, *42*, 2186–2188. (f) Bohle, D. S.; Chen, W.-C.; Hung, C.-H. *Inorg. Chem.* **2002**, *41*, 3334–3336. (g) Furuta, H.; Ogawa, T.; Uwatoko, Y.; Araki, K. *Inorg. Chem.* **1999**, *38*, 2676–2682. (h) Ogawa, T.; Furuta, H.; Takahashi, M.; Morino, A.; Uno, H. *J. Organomet. Chem.* **2000**, *611*, 551–557. (4) (a) Furuta, H.; Ishizuka, T.; Osuka, A. *J. Am. Chem. Soc.* **2002**, *124*, 5622–5623. (b) Harvey, J. D.; Ziegler, C. J. *Chem. Commun.* **2002**, 1942–1943. (c) Chen, W.-C.; Hung, C.-H. *Inorg. Chem.* **2001**, *40*, 5070–5071. (d) Hung, C.-H.; Chen, W.-C.; Lee, G.-H.; Peng, S.-M. *Chem. Commun.* **2002**, 1516–1517.

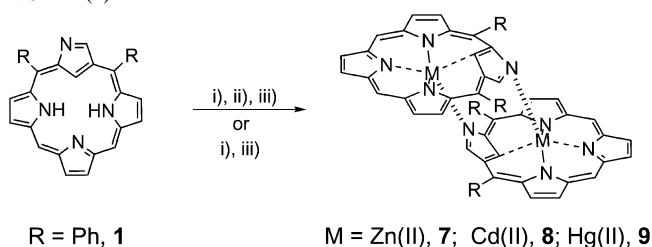
**Chart 2.** Structures of N-Confused Porphyrins and Normal Porphyrins


complexes have been also synthesized with Rh(I)<sup>5</sup> (Chart 1c), and the combination of both inner and outer coordination was seen in the dimer complexes of Pd(II)<sup>3d</sup>, Zn(II),<sup>4a</sup> Mn(II),<sup>4b</sup> and Fe(II).<sup>4d</sup>

Previously, we showed the facile formation of a mutually coordinating Zn(II) dimer complex of N-confused tetraphenylporphyrin (NCTPP, **3**) in solution.<sup>4a</sup> Thereafter, the crystal structures of dimeric Mn(II)<sup>4b</sup> and Fe(II)<sup>4d</sup> NCP complexes were reported by Ziegler's and Hung's groups, respectively. However, a comparison of these structures with the Zn(II) complex in solution was unfeasible owing to the paramagnetism of the Mn(II) and Fe(II) species. Thus, the question of the exact structure of the Zn(II) complex remained unanswered. Herein, we report the first X-ray structures of air-stable dimeric Zn(II) and Cd(II) NCP complexes (**7**, **8**) in addition to the <sup>1</sup>H NMR spectra of **7**, **8**, and the Hg(II) complex (**9**). For crystallographic reasons, the less crowded NCP derivative, 5,20-diphenyl-NCP (NCDPP, **1**),<sup>6</sup> was investigated in this work (Chart 2). The structures of the dimer complexes with group 12 metals are similar to the Fe(II) and Mn(II) complexes with the exception of the relative orientation of the two *confused* pyrrole rings. The thermodynamic parameters of the monomer ligand exchange reactions between dimer complexes as well as the metal-transfer reaction from the Zn(II) NCP complex to a *normal* porphyrin are also reported.

## Results and Discussion

**Preparation of Zn(II), Cd(II), and Hg(II) Dimer Complexes (7–9).** The Zn(II), Cd(II), and Hg(II) NCDPP dimer complexes (**7–9**) were prepared by using **1** and the corresponding metal acetates in CH<sub>2</sub>Cl<sub>2</sub> (Scheme 1). For example, the Zn(II) complex (**7**) was obtained by stirring a mixture of **1** and Zn(OAc)<sub>2</sub>·2H<sub>2</sub>O at room temperature for 2 h. After washing with 1% aqueous Et<sub>4</sub>NOH, complex **7** was crystallized from a CH<sub>2</sub>Cl<sub>2</sub>/hexane solution (81% yield). The Cd(II) complex (**8**) was synthesized from **1** and Cd(OAc)<sub>2</sub>·2H<sub>2</sub>O in 83% yield by a similar method except for a longer reaction time (2 days). Under the same reaction conditions, NCTPP (**3**) yielded the corresponding Cd(II) dimer complex in only a 60% yield, suggesting the higher reactivity of the less crowded ligand **1**. The formation process of the Cd(II) complex was apparently different from that of the Zn(II) dimer. In the case of Zn(II), a tetranuclear dimer

**Scheme 1.** Syntheses of Dimer Metal Complexes (**7–9**) of NCDPP (**1**)<sup>a</sup>


<sup>a</sup> Key: (i) M(OAc)<sub>2</sub>·2H<sub>2</sub>O (M = Zn, Cd) or Hg(OAc)<sub>2</sub>, CH<sub>2</sub>Cl<sub>2</sub>; (ii) 1% Et<sub>4</sub>NOH(aq); (iii) crystallization from CH<sub>2</sub>Cl<sub>2</sub>/hexane.

complex was formed initially, which was transformed into a dinuclear complex after treatment with an alkaline solution.<sup>4a</sup> In the case of the Cd(II) complex, direct formation of **8** was suggested from the absorption spectral change during the reaction. Similarly, the Hg(II) complex (**9**) was obtained without alkali treatment using 1 equiv of Hg(OAc)<sub>2</sub> in refluxed CH<sub>2</sub>Cl<sub>2</sub>. When 2 equiv of Hg(OAc)<sub>2</sub> was used under the same conditions as those of the Cd(II) complex, a complicated mixture was produced. In the case of the Hg(II) complex, the dimer was not isolated due to its inherent instability, but the formation of structure of **9** was unambiguously confirmed by the <sup>1</sup>H NMR analysis.

The dimer structures of **7** and **8** were explicitly elucidated by single-crystal X-ray analyses (Figure 1a,b and Table 1). In accordance with the predicted structure of the Zn(II) NCTPP complex,<sup>4a</sup> the two Zn(II) metals in **7** are coordinated with the N<sub>3</sub>C core and the outer N of the other NCDPP in a pair, respectively. The structures of the Zn(II) and Cd(II) dimer complexes are nearly equivalent and, interestingly, are similar to the Mn(II) and Fe(II) complexes (Figure 1c) except for the relative orientation of the *confused* pyrrole rings, i.e., a molecular symmetry of C<sub>2</sub> for **7** and **8** and C<sub>i</sub> for the Mn(II) and Fe(II) complexes. In other words, the dimers **7** and **8** are formed with two NCP rings of the same chirality while the Mn(II) and Fe(II) complexes consist of both enantiomers in a molecule. In the crystals, two *confused* pyrrole rings in **7** (and **8**) are tilted by 47.5(3) and 49.9(3)° (41.3(5) and 42.9(5)°) from the corresponding N<sub>3</sub> mean plane comprising the three inner nitrogen atoms. The Zn atoms of **7** (and Cd of **8**) are separated from each other by a distance of 5.217(2) Å (5.230(2) Å) and located 0.61(1) and 0.64(1) Å (0.87(1) and 0.85(1) Å) above the mean planes, respectively, with an average N–Zn (and N–Cd) distance of 2.07(1) Å (2.24(1) Å). Furthermore, the distance between the inner carbon and the nearest Zn (Cd) atom, 2.53(1) Å (2.57(1) Å), is short enough for a side-on η<sup>1</sup>-coordination.

**Structures of Dimer Complexes in Solution.** The similarity of the structure of the Cd(II) dimer complex to the Zn(II) complex in solution was inferred from the analogous profile of the absorption spectra (Figure 2). Namely, a broad Soret-like band and strong Q-band at the longest wavelength were observed at 447 and 738 nm and 459 and 741 nm for **7** and **8**, respectively. In fact, the <sup>1</sup>H NMR spectrum of **7** in CDCl<sub>3</sub> showed the inner and outer CH signals (H<sup>1</sup>, H<sup>2</sup>) at –3.99 and 2.57 ppm, respectively (Figure 3 (top)), and the corresponding signals of **8** and **9** were observed in almost

(5) Srinivasan, A.; Furuta, H.; Osuka, A. *Chem. Commun.* **2001**, 1666–1667.

(6) Furuta, H.; Morimoto, T.; Osuka, A. *Org. Lett.* **2003**, *5*, 1427–1430.

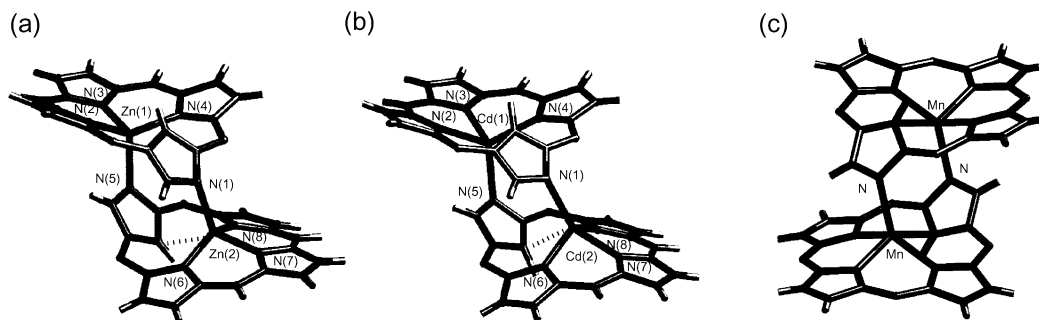


**Figure 1.** Dimer structures of (a) Zn(II) NCDPP (**7**), (b) Cd(II) NCDPP (**8**), and (c) Ziegler's Mn(II) complex. The phenyl groups and solvent molecules are omitted for clarity. Selected bond lengths (Å) for **7**: Zn(1)–N(5), 2.062(9); Zn(1)–N(2), 2.145(6); Zn(1)–N(3), 2.012(7); Zn(1)–N(4), 2.103(8); Zn(2)–N(1), 2.060(8); Zn(2)–N(6), 2.134(8); Zn(2)–N(7), 1.992(7); Zn(2)–N(8), 2.098(6). Selected bond lengths (Å) for **8**: Cd(1)–N(5), 2.23(2); Cd(1)–N(2), 2.28(1); Cd(1)–N(3), 2.20(1); Cd(1)–N(4), 2.25(1); Cd(2)–N(1), 2.21(2); Cd(2)–N(6), 2.28(1); Cd(2)–N(7), 2.21(1); Cd(2)–N(8), 2.25(1). Note: Mn(II) structure **c** was taken from ref 4b-reproduced by permission of The Royal Society of Chemistry.

**Table 1.** Crystal Data for Zn(II)– and Cd(II)–NCDPP Dimer Complexes (**7**, **8**)

	<b>7</b> ·2CH <sub>2</sub> ClCH <sub>2</sub> Cl	<b>8</b> ·C <sub>6</sub> H <sub>14</sub>
empirical formula	C <sub>68</sub> H <sub>48</sub> N <sub>8</sub> Zn <sub>2</sub> Cl <sub>4</sub>	C <sub>70</sub> H <sub>54</sub> N <sub>8</sub> Cd <sub>2</sub>
fw	1249.75	1232.07
space group (No.)	<i>P</i> 1̄ (No. 2)	<i>P</i> 1̄ (No. 2)
cryst syst	triclinic	triclinic
<i>a</i> , Å	13.9012(4)	12.379(8)
<i>b</i> , Å	14.5110(3)	15.64(1)
<i>c</i> , Å	16.5462(4)	17.46(1)
α, deg	67.493(4)	63.24(6)
β, deg	81.366(3)	78.22(6)
γ, deg	63.664(5)	67.43(6)
<i>V</i> , Å <sup>3</sup>	2762.7(2)	2784.9(3)
<i>T</i> , °C	–150	–150
<i>Z</i>	2	2
<i>D</i> <sub>calcd</sub> , g cm <sup>–3</sup>	1.502	1.469
cryst size, mm	0.40 × 0.40 × 0.18	0.20 × 0.20 × 0.10
θ, deg	27.5	27.4
no. of reflns measd	12 164	8592
no. of reflns obsd	10 192	4499
radiatn λ, Å	0.710 69 (Mo Kα)	0.710 75 (Mo Kα)
μ(Mo Kα), cm <sup>–1</sup>	11.149	8.167
GOF ( <i>I</i> > 3σ( <i>I</i> ))	1.378	0.991
<i>R</i> <sup><i>a</i></sup> ( <i>I</i> > 3σ( <i>I</i> ))	0.089	0.085
<i>R</i> <sub>w</sub> <sup><i>b</i></sup>	0.121	0.110

$$^a R = \frac{\sum ||F_o| - |F_c||}{\sum |F_o|}, \quad ^b R_w = \frac{[\sum w(|F_o| - |F_c|)^2 / \sum |F_o|^2]^{1/2}}{}$$

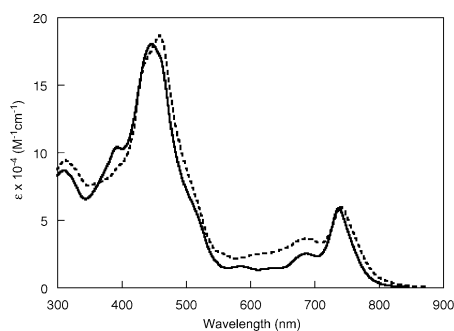


**Figure 2.** Absorption spectra of **7** (solid line) and **8** (broken line) in CH<sub>2</sub>-Cl<sub>2</sub>.

the same region (Figure 3 (middle, bottom)). One significant difference is the outer CH signals at 3.44 and 3.60 ppm for **8** and **9**, respectively, which are shifted downfield by ca. 1 ppm compared with **7**. This is attributable to the weaker ring current effect due to the longer distance between the NCP planes in the dimer.<sup>7</sup> Furthermore, the magnetic coupling between the nuclear spin of the outer N-coordinated metal M<sub>N</sub> (M = Cd, Hg) and the outer CH (H<sup>2</sup>) was observed as

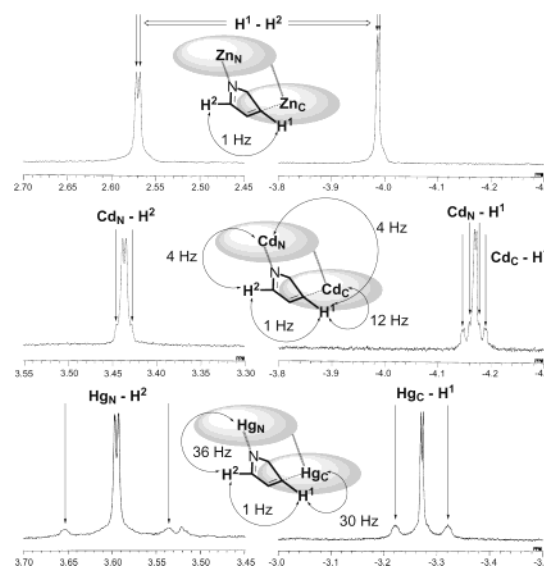


**Figure 3.** <sup>1</sup>H NMR spectra (300 MHz, 25 °C, CDCl<sub>3</sub>) of Zn(II) (**7**, top), Cd(II) (**8**, middle), and Hg(II) (**9**, bottom) complexes.

satellite doublet signals with *J* = 4 and 36 Hz in **8** and **9**, respectively. In the upfield region, the doublet inner CH (H<sup>1</sup>) signals at –4.15 and –3.27 ppm for **8** and **9**, respectively, were also associated with satellite doublet signals (*J* = 12 and 30 Hz) assignable to the coupling between inner CH and η<sup>1</sup>-coordinated metal (M<sub>C</sub>) of Cd(II) and Hg(II), respectively.<sup>8,9</sup> In complex **8**, the shoulder signals with *J* = 4 Hz were associated with the same H<sup>1</sup> signal, which was interpreted as a coupling with the Cd<sub>N</sub> metal in the partner NCP ring. This long-range coupling is direct evidence for dimer formation in solution.<sup>10</sup> Correlations of the mutual magnetic couplings are summarized in Figure 3.

- (7) In the single crystal, the distances between the N<sub>3</sub> mean plane and the outer α-carbon of the opposite NCP for the Zn complex (**7**) are 3.005(9) and 3.082(9) Å, which are shorter than those of the Cd complex (**8**), 3.20(2) and 3.12(2) Å.
- (8) A similar Cd–H coupling (*J*<sub>Cd–H</sub> = 4.4 Hz) was reported in the tetraphenyl-*p*-benzporphyrin: Stepien, M.; Latos-Grażyński, L. *J. Am. Chem. Soc.* **2002**, *124*, 3838–3839.
- (9) Although M<sub>N</sub> is equivalent to M<sub>C</sub>, the two center metals are distinguished here as a matter of convenience.
- (10) The formation of complexes **7** and **8** in solution was also supported from vapor pressure osmometry (VPO), which showed the dimer molecular weight at 976 ± 78 (calcd 1052) and 1101 ± 88 (calcd 1146) g/mol, respectively.

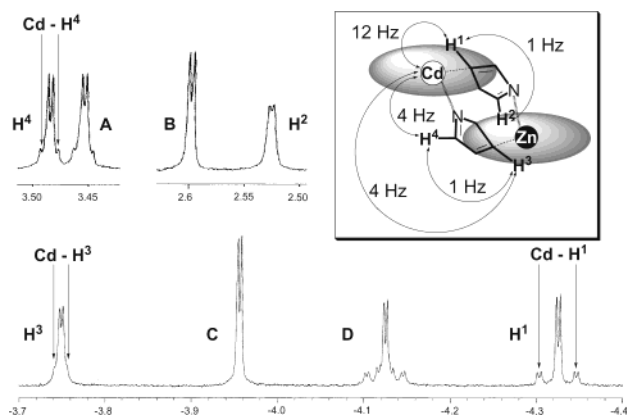


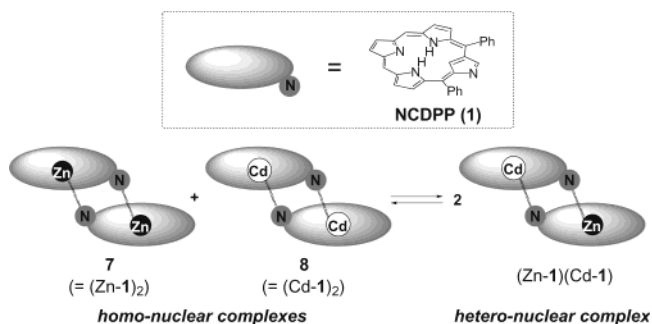
**Figure 4.**  $^1\text{H}$  NMR signals of a mixed solution of **7** and **8** (1:1, 2 mM each) in  $\text{CDCl}_3$  at 50  $^\circ\text{C}$ . **A–D** represent the outer CH signals of **8** and **7** and the inner CH signals of **7** and **8**, respectively.

The chemical shift differences ( $\Delta\delta$ ) between the signals at the both ends in the  $^1\text{H}$  NMR spectra are 12.7, 12.9, and 11.9 ppm for **7–9**, respectively. The smaller  $\Delta\delta$  value observed in **9** is probably due to the loose dimer structure as the result of the larger ion radius of  $\text{Hg}(\text{II})$ . Support for the  $\eta^1$ -interaction between the  $\text{sp}^2$  inner carbon atoms and the center metals in **8** and **9** was obtained from the  $^{13}\text{C}$  NMR spectra.<sup>11</sup> Specifically, the  $^{13}\text{C}$  signals of the inner carbons of **8** and **9** were observed at 76.0 and 86.5 ppm, respectively; these are closer to the value of the  $\text{sp}^2$  hybridized inner carbon atom's signal (99.0 ppm) in the free base **1** than that of the inner  $\text{sp}^3$ -hybridized carbon (34.1 ppm) of the inner-C alkylated NCTPP  $\text{Ni}(\text{II})$  complex.<sup>12</sup>

**Ligand Exchange Equilibrium in Solution.** As described above, the dimer complexes use both the inner and outer coordination sites simultaneously. The tetradentate macrocycle will clearly bind metals more strongly than the monodentate outer coordination site. To evaluate the stability of these dimers in solution, the solution equilibria in several mixed dimer systems were examined.

At first, the complexes **7** and **8** were mixed and stirred for 0.5 h at room temperature in  $\text{CDCl}_3$ . The dimer equilibrium was then analyzed directly from the  $^1\text{H}$  NMR spectra. As shown in Figure 4, apart from the original signals (**A–D**), the resulting solution exhibits new signals ( $\text{H}^1$ – $\text{H}^4$ ) bearing Cd–H couplings of a heterodimer complex containing both  $\text{Zn}(\text{II})$  and  $\text{Cd}(\text{II})$  metals. The most upfield-shifted signal at  $-4.32$  ppm ( $\text{H}^1$ ) is assignable to the inner CH of the NCP ring containing the  $\text{Cd}(\text{II})$  ion as judged by the small double doublet signals ( $J = 12$  and 1 Hz). The other shoulder signals seen in **8** are not observed due to the lack of  $\text{Cd}(\text{II})$  ion in the paired NCP ring (compare the  $\text{H}^1$  signal with the signal **D**). Instead, the signal at  $-3.75$  ppm ( $\text{H}^3$ ), assignable to the inner CH of the NCP ring having  $\text{Zn}(\text{II})$ , has a shoulder due to the long-range coupling with the  $\text{Cd}(\text{II})$  ion in the partner NCP ring. Here, the strong NOE correlation between two outer protons ( $\text{H}^2$  and  $\text{H}^4$ ) also supports the  $C_2$  arrange-

**Scheme 2.** Ligand Exchange Equilibrium of a Mixed Solution of **7** and **8**



ment of the two *confused* pyrrole rings in solution, consistent with the solid state.<sup>13</sup>

In the solution of **7** and **8**, the monomer species were detected neither by  $^1\text{H}$  NMR nor absorption spectroscopy. As the shape of the absorption spectra did not change even at a low concentration around  $10^{-5}$  M, the concentration of the monomer species should be extremely low. Assuming that the dimers **7** and **8** are in equilibrium as shown in the Scheme 2, the equilibrium constant ( $K$ ) was estimated to be 2.5 and 2.7 at 25 and 50  $^\circ\text{C}$ , respectively. Because the  $K$  values are lower than 4, the value expected from only the mixing entropy term,<sup>14</sup> the stability of the heteronuclear dimer should be smaller than homodimers. Supporting this, the thermodynamic parameters ( $\Delta H$  and  $\Delta S$ ) were estimated at 0.68 kJ/mol and 10 J/(K mol), respectively, from the van't Hoff plots. The positive  $\Delta H$  value indicates the relatively unfavorable formation of the heteronuclear dimer complex, which is probably attributable to the distortion of the dimer structure due to the difference of outer N coordination of both NCP rings. The  $\Delta S$  value is nearly equal to the statistical value ( $R \ln 4 = 11.5$  J/(K mol), where  $R$  is gas constant). From these values, it is clear that the dominant formation of the heteronuclear dimer complex in the equilibrium is attributable to the larger entropy term ( $T\Delta S > \Delta H$ ).

Similarly, the corresponding heteronuclear dimers were also produced by mixing the complexes of  $\text{Zn}(\text{II})$  (**7**) and  $\text{Hg}(\text{II})$  (**9**), as well as  $\text{Cd}(\text{II})$  (**8**) and  $\text{Hg}(\text{II})$  (**9**). In contrast with the heterodimer derived from **7** and **8**, the ligand exchange process is relatively slow and requires more harsh conditions in both the cases. Specifically, the equilibrium constant after mixing for 0.5 h was estimated as  $K = 0.3$  at 25  $^\circ\text{C}$ , but the final equilibrium states had  $K = 0.6$  and 1.3 at 25  $^\circ\text{C}$ , respectively; these states were accomplished by additional stirring at 50  $^\circ\text{C}$  for 1 h. These results indicate that the heteronuclear complexes containing  $\text{Hg}(\text{II})$  ion are less stable compared to those of  $\text{Zn}(\text{II})$  or  $\text{Cd}(\text{II})$ , probably due to the imbalance of the ion sizes. On the other hand, introduction of additional *meso*-phenyl groups did not affect the equilibrium process so much as judged by the  $^1\text{H}$  NMR

(11) The  $^{13}\text{C}$  signal of Zn dimer **7** was not obtained due to the poor solubility. However, the corresponding signal of the  $\text{Zn}(\text{II})$  NCTPP dimer complex (**10**) was observed at 78.3 ppm.<sup>4a</sup>

(12) Schmidt, I.; Chmielewski, P. J. *Chem. Commun.* **2002**, 92–93.

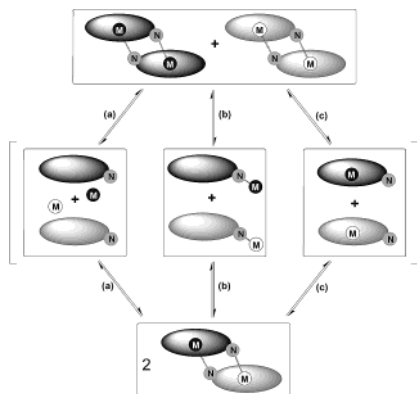
(13) In the present crystal structures, the distances between the two outer CH carbons of the dimers are 3.26(1) and 3.18(2) Å for the  $\text{Zn}(\text{II})$  and  $\text{Cd}(\text{II})$  complexes, respectively, while the two carbons of Ziegler's Mn dimer complex are separated by 4.99(1) Å. See the Supporting Information.

(14) Kaim, W.; Klein, A.; Glöckle, M. *Acc. Chem. Res.* **2000**, *33*, 755–763.

**Table 2.** Equilibrium Constants ( $K$ ) between Homo- and Heteronuclear Dimer Complexes at 25 °C in CDCl<sub>3</sub><sup>a</sup>

homonuclear complexes	$K$	hetero-nuclear (or ligand) complex
7 + 8	2.5	(Zn-1)(Cd-1)
8 + 9	1.3	(Cd-1)(Hg-1)
9 + 7	0.6	(Hg-1)(Zn-1)
10 + 7	3.8	(Zn-3)(Zn-1)

<sup>a</sup> 1: NCDPP. 3: NCTPP. 7: (Zn-1)<sub>2</sub>. 8: (Cd-1)<sub>2</sub>. 9: (Hg-1)<sub>2</sub>. 10: (Zn-3)<sub>2</sub>.

**Scheme 3.** Three Possible Mechanisms for the Formation of a Heteronuclear Dimer Complex

analyses of a mixture solution of Zn(II) NCDPP (7) and Zn(II) NCTPP (10), where the exchange reaction was as fast as that of 7 and 8 and had an equilibrium constant  $K = 3.8$  at 25 °C. This is almost same as the statistical value 4, which suggests that  $\Delta H$  of this heterodimer formation is nearly equal to zero; namely, the homo- and heterodimer have the same stability. The  $K$  values obtained are summarized in Table 2.

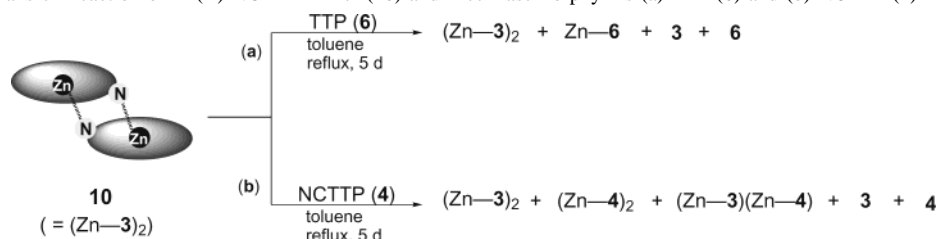
The above results indicate that the formation of heteronuclear NCP dimer is general for these complexes with group 12 metals. Mechanistically, three possible schemes can be considered in the dimer formation process according to the sites of coordinated metal bound. The first one is a free metal exchange reaction in which two metals are rapidly exchanging in the dimer complex and behave as if metal ions are unbound (Scheme 3a). The second one is a free monomer ligand exchange at the core, in which a metal is bound tightly at the outer N site (Scheme 3b), and the third one is the ligand exchange at the core where the metal is bound in the core (Scheme 3c). To clarify the mechanism, a cross experiment was performed by using a mixture of Zn(II) 5,20-di-*p*-tolyl-NCP dimer (11) and Cd(II) NCDPP complex (8). If the reaction proceeds in the first mechanism, 16 kinds of inner CH signals from 10 dimer complexes should appear in the upfield region. However, just like the system of 7 and

8, the obtained spectra showed only four sets of inner CH signals, which were assignable to the starting dimer complexes (8 and 11) and a heterodimer consisting of the monomer ligands derived from both the homodimer complexes (Figure 5). In the second mechanism, the newly formed dimer should consist of a set of monomer of (Cd-2) and (Zn-1) moieties; on the other hand, in the third mechanism, the combination should be that of (Zn-2) and (Cd-1) parts. The detailed comparison of the chemical shifts of the inner CH signals of H<sup>1</sup> and H<sup>3</sup> in Figure 5 with those of (Zn-1)(Cd-1) and (Zn-2)(Cd-2) strongly indicates that the newly formed dimer consists of (Zn-2) and (Cd-1) moieties, which is fully consistent with the third mechanism.<sup>15</sup> This result implies that the inner coordinated metals are tightly bound by each of the NCP inner core and not exchangeable in the dimer complex. In solution, both outer nitrogens dissociate metals of paired NCP rings more readily<sup>16</sup> and exchange the monomer parts in forming a new dimer complex.

**Metal-Transfer Reactions.** Compared with a square-planar complex of a normal porphyrin, the present nonplanar NCP complexes are expected to coordinate and release metal ions readily because of the weak side-on  $\eta^1$ -coordination of the sp<sup>2</sup> carbon in the core. This would be an advantage when using NCP for a metalation catalyst or metal carrier. To examine this possibility, we treated the Zn(II) NCP complex with a free base porphyrin as a metal acceptor.

In the control experiment, a toluene solution of the Zn(II) complex of TPP (5,10,15,20-tetraphenylporphyrin, 5) and free base TTP (5,10,15,20-tetra-*p*-tolylporphyrin, 6) was refluxed for 5 days but the composition of the solution did not change at all. On the other hand, when Zn(II) dimer complexes of NCTPP (3) and free base TTP (6) were stirred under the same conditions, the Zn(II) complex of 6 and the free base NCTPP (3) as well as the starting two species were detected by <sup>1</sup>H NMR (Figure 6a). The production of the Zn(II) complex of 6 was confirmed by the  $\beta$ -proton signals at 8.96 ppm. This is clear evidence that the center Zn(II) ion of NCP was released and transferred to the free base porphyrin.

Similarly, the metal-transfer reaction of Zn(II) NCTPP complex (10) to free base NCTTP (N-confused 5,10,15,20-tetra(*p*-tolyl)porphyrin, 4) was examined under the same conditions. In the <sup>1</sup>H NMR spectrum, the inner CH signals of NCTPP and NCTTP as well as the inner CH signals of the Zn(II) complexes of NCTPP and NCTTP were observed in the region from -3.5 to -5.0 ppm. The other signals were assigned to the heteronuclear dimer complex (Figure 6b).

**Scheme 4.** Metal-Transfer Reaction of Zn(II) NCTPP Dimer (10) and Free Base Porphyrins (a) TTP (6) and (b) NCTTP (4)

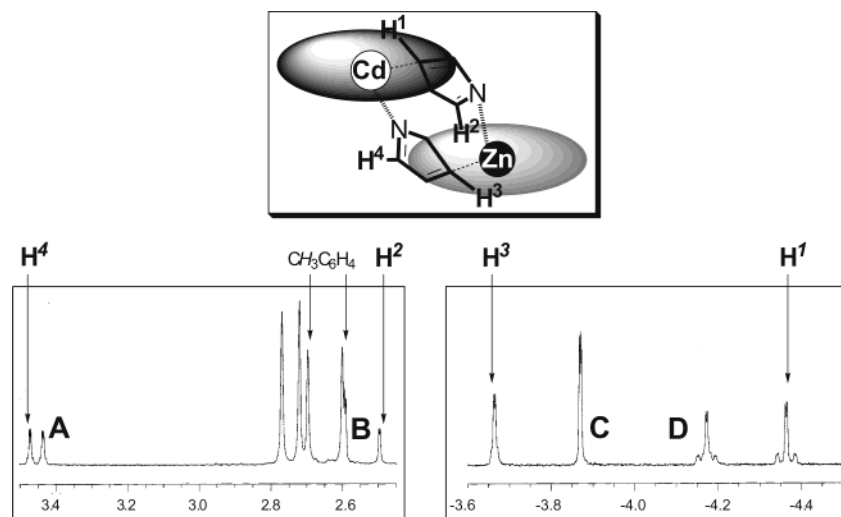


**Figure 5.**  $^1\text{H}$  NMR (300 MHz, 25 °C,  $\text{CDCl}_3$ ) signals of a mixture of **8** and **10** (1:1, 2 mM each). **A** and **B** represent the outer CH signals of **8** and **10**, and **C** and **D** the inner CH signals of **10** and **8**, respectively.

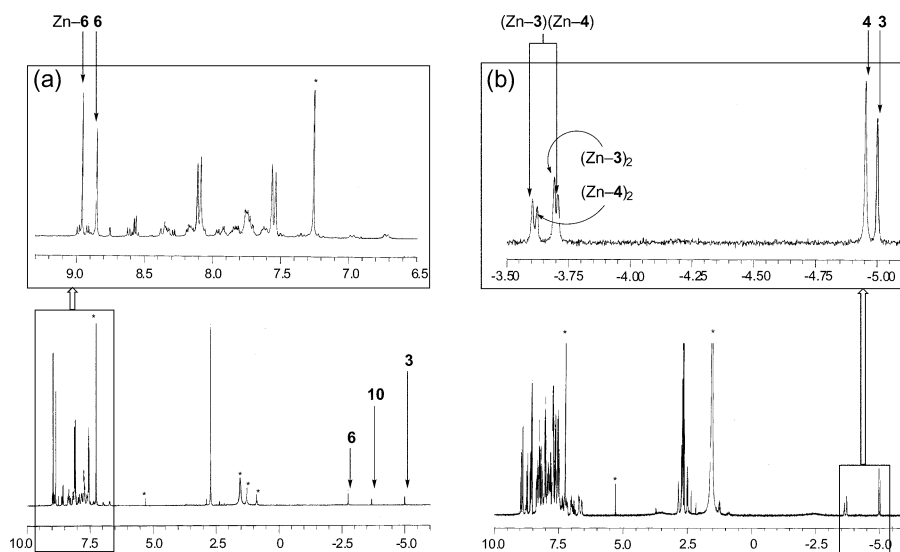


**Figure 6.**  $^1\text{H}$  NMR spectra after metal-transfer reactions of Zn(II) NCTPP dimer (**10**) and free base porphyrins (a) TTP (**6**) and (b) NCTTP (**4**).

This result indicates that the center Zn(II) ion in the dimer complex was transferred to the other NCP free base, producing the corresponding dimer complex and successively exchanging their monomer parts with one another at toluene refluxing temperature.

## Conclusion

N-confused porphyrin forms dimer complexes with group 12 metals in which the metal ions are coordinated by the three inner nitrogens as well as one carbon in the core and the outer nitrogen of the paired NCP, respectively, in the

- (15) The inner CH signals of (Zn-1) in (Zn-1)(Cd-1) and (Zn-2) in (Zn-2)(Cd-2) were observed at -3.79 and -3.66 ppm at 25 °C, respectively. On the other hand, the inner CH signals of (Cd-1) in (Zn-1)(Cd-1) and (Cd-2) in (Zn-2)(Cd-2) were observed at -4.38 and -4.25 ppm at 25 °C, respectively. Assuming that the chemical shift difference is mainly due to the change of *meso*-aryl groups, the signal at -3.66 ppm in Figure 5 is assignable to the inner CH proton of (Zn-2) and the signal at -4.36 ppm to that of (Cd-1). See the Supporting Information.
- (16) In fact, analyses of the dimer complexes by FABMS or MALDI-TOF-MS showed the signal corresponding to the monomer part with the center metal.

solid state and in solution. Reflecting the weaker binding ability of the outer nitrogen, the dimer complexes of different metals can readily exchange their monomer parts with one another, forming heteronuclear dimer complexes. The equilibrium constants of the exchange reaction and the stability of the dimer complexes depend largely on the coordinated metal ions. Furthermore, the center metal ions can be removed and transferred to the other porphyrin cores.

Conceptually, the dynamic exchange of the monomer partner by the reversible coordination of the present system can be considered as a type of “porphyrin metathesis”. By the *recombination* of the dimer species, the information of one molecule can be transferred to the other. As a lot of information could be implanted on this type of dimer complex by using various ligands, enriched nuclear spin, different metals, and so on, we think the present system is promising for a variety of applications in the area of *supramolecular informatics chemistry*.<sup>17</sup>

(17) Glaser, S. J. *Angew Chem., Int. Ed.* **2001**, *40*, 147–149.

## Experimental Section

**Materials.** Free base 5,20-NCDPP (**1**) and N-confused 5,20-di-*p*-tolyl-NCP (**2**) for the dimer complex **11** were synthesized with the corresponding 2,4-bis(arylhydroxymethyl)pyrrole and *meso*-unsubstituted tripyrrane by a [3 + 1] acid-catalyzed condensation reaction, followed by oxidation.<sup>6</sup> Free base NCTPP (**3**) and NCTTP (**4**) were prepared as described before.<sup>18</sup> Commercially available reagents and solvents were used without further purification.

**Instrumentation.** <sup>1</sup>H NMR and <sup>13</sup>C NMR spectra were recorded on a JEOL JNM-AL270 FT NMR system operating at 300 MHz for <sup>1</sup>H NMR and 75.5 MHz for <sup>13</sup>C NMR. The residual <sup>1</sup>H NMR and <sup>13</sup>C NMR resonances of the deuterated solvents were used as the internal reference. UV/visible spectra were recorded on a Shimadzu UV-3150 spectrometer. Vapor pressure osmometry (VPO) data were obtained on a Gonotec Osmomat 070.

**X-ray Crystallography.** The crystal data for **7** and **8** are listed in detail in Table 1. Single crystals of **7** and **8** were obtained by vapor diffusion of hexane into a CH<sub>2</sub>ClCH<sub>2</sub>Cl solution of **7** and a CH<sub>2</sub>Cl<sub>2</sub> solution of **8**, respectively. All measurements were made on a Rigaku Raxis Rapid imaging plate area detector with graphite-monochromated Mo K $\alpha$  radiation. The structures were solved by direct methods<sup>19</sup> for **7** and heavy-atom Patterson methods<sup>20</sup> for **8** and expanded using Fourier techniques.<sup>21</sup> Some non-hydrogen atoms were refined anisotropically, while the rest were refined isotropically. Hydrogen atoms were refined using the standard riding model.<sup>22</sup>

**Determination of the Equilibrium Constant *K*.** *K* values were evaluated as  $[\text{heterodimer}]^2/([\text{homodimer 1}][\text{homodimer 2}])$  for the mixture system of homodimer 1 and homodimer 2. If one takes into account the dimension of the constant, it can be substituted by  $I_{\text{hetero}}^2/(I_{\text{homo1}}I_{\text{homo2}})$ , where *I* is the integral value for a particular signal. In this study, we employed the signals of the inner CH proton of the confused pyrrole ring because they appear far apart enough to be distinguished from each other in the <sup>1</sup>H NMR spectra.

**Zn(II) Dimer Complex of 2-Aza-5,20-diphenyl-21-carbaporphyrin (7).** NCDPP (**1**) was treated with 2 equiv of Zn(OAc)<sub>2</sub>·2H<sub>2</sub>O in CH<sub>2</sub>Cl<sub>2</sub>. After 2 h, the reaction mixture was washed with

1% Et<sub>3</sub>NOH aqueous solution and water twice. The solvent was removed in vacuo, and the obtained solid was recrystallized from CH<sub>2</sub>Cl<sub>2</sub>/hexane to afford a green solid (81% yield). <sup>1</sup>H NMR (300 MHz, 25 °C, CDCl<sub>3</sub>, ppm):  $\delta$  8.70 (s, 2H, *meso*-H), 8.60 (d, *J* = 4.2 Hz, 2H,  $\beta$ -H), 8.43 (d, *J* = 4.8 Hz, 2H,  $\beta$ -H), 8.40 (d, *J* = 4.5 Hz, 2H,  $\beta$ -H), 8.35 (d, *J* = 4.5 Hz, 2H,  $\beta$ -H), 8.23 (d, *J* = 4.2 Hz, 2H,  $\beta$ -H), 8.22 (s, 2H, *meso*-H), 8.08 (d, *J* = 4.8 Hz, 2H,  $\beta$ -H), 7.72–7.43 (m, 16H, Ph), 6.68 (br, 4H, Ph), 2.57 (d, *J* = 1.2 Hz, 2H, outer  $\alpha$ -H), –3.99 (d, *J* = 1.2 Hz, 2H, inner CH). UV/vis (CH<sub>2</sub>Cl<sub>2</sub>;  $\lambda_{\text{max}}$ , nm (10<sup>–4</sup> $\epsilon$ ): 311 (8.62), 394 (10.3), 447 (18.0), 584 (1.58), 687 (2.51), 738 (5.86). VPO: 976  $\pm$  78 g/mol (calcd 1052 g/mol).

**Cd(II) Dimer Complex of 2-Aza-5,20-diphenyl-21-carbaporphyrin (8).** NCDPP (**1**) was treated with 2 equiv of Cd(OAc)<sub>2</sub>·2H<sub>2</sub>O in CH<sub>2</sub>Cl<sub>2</sub> for 2 days. After a workup identical with that described above or without base treatment, the residue was recrystallized from CH<sub>2</sub>Cl<sub>2</sub>/hexane twice to afford a green product (83% yield). <sup>1</sup>H NMR (300 MHz, 25 °C, CDCl<sub>3</sub>, ppm):  $\delta$  8.77 (s, 2H, *meso*-H), 8.63 (d, *J* = 4.5 Hz, 2H,  $\beta$ -H), 8.60 (s, 2H, *meso*-H), 8.54 (d, *J* = 4.5 Hz, 2H,  $\beta$ -H), 8.45 (d, *J* = 4.5 Hz, 2H,  $\beta$ -H), 8.41 (d, *J* = 3.6 Hz, 2H,  $\beta$ -H), 8.40 (d, *J* = 3.6 Hz, 2H,  $\beta$ -H), 8.07 (d, *J* = 4.5 Hz, 2H,  $\beta$ -H), 7.74–7.23 (m, 16H, Ph), 6.56 (br, 4H, Ph), 3.44 (d, *J* = 1.2 Hz, 2H, outer  $\alpha$ -H), –4.17 (d, *J* = 1.2 Hz, 2H, inner CH). UV/vis (CH<sub>2</sub>Cl<sub>2</sub>;  $\lambda_{\text{max}}$ , nm (10<sup>–4</sup> $\epsilon$ ): 313 (9.31), 459 (18.3), 687 (3.69), 741 (5.86). VPO: 1101  $\pm$  88 g/mol (calcd 1146 g/mol).

**Hg(II) Dimer Complex of 2-Aza-5,20-diphenyl-21-carbaporphyrin (9).** NCDPP (**1**) was treated with 1 equiv of Hg(OAc)<sub>2</sub> in refluxing CH<sub>2</sub>Cl<sub>2</sub> for 1.5 days. After a workup identical with that described in **8**, the residue was recrystallized from CH<sub>2</sub>Cl<sub>2</sub>/hexane several times to afford the brown product, which was contaminated at least by **1**. <sup>1</sup>H NMR (300 MHz, 25 °C, CDCl<sub>3</sub>, ppm):  $\delta$  8.58 (d, *J* = 4.5 Hz, 2H,  $\beta$ -H), 8.56 (s, 2H, *meso*-H), 8.48 (d, *J* = 4.5 Hz, 2H,  $\beta$ -H), 8.42 (s, 2H, *meso*-H), 8.27–8.24 (m, 6H,  $\beta$ -H), 7.97 (d, *J* = 4.5 Hz, 2H,  $\beta$ -H), 7.72–7.21 (m, 12H, Ph), 6.84–6.35 (br, 8H, Ph), 3.60 (d, *J* = 1.2 Hz, 2H, outer  $\alpha$ -H), –3.27 (d, *J* = 1.2 Hz, 2H, inner CH).

In both **8** and **9**, all the signals except those of the phenyl groups are coupled with Cd(II) and Hg(II). To avoid the complication, the data of heteroatom couplings are not shown here (see Supporting Information Figures S2 and S3).

**Supporting Information Available:** Crystallographic data (CIF) and ORTEP drawings for **7** and **8**, <sup>1</sup>H NMR spectra of **7–9**, a van't Hoff plot for the exchange reaction of **7** and **8**, <sup>1</sup>H NMR spectra of mixture solutions of **7/8**, **8/9**, **9/7**, and **10/7**, an NOE difference <sup>1</sup>H NMR spectrum of mixture solutions of **7** and **8**, and an <sup>1</sup>H NMR spectrum of mixture solutions of **8–11** with spectra of (Zn–1)(Cd–1) and (Zn–2)(Cd–2). This material is available free of charge via the Internet at <http://pubs.acs.org>.

IC035294E

- (18) Geier, G. R., III; Haynes, D. M.; Lindsey, J. S. *Org. Lett.* **1999**, *1*, 1455–1458.
- (19) SIR97: Altomare, A.; Burla, M.; Camalli, M.; Cascarano, G.; Giacovazzo, C.; Guagliardi, A.; Moliterni, A.; Polidori, G.; Spagna, R. *J. Appl. Crystallogr.* **1999**, *32*, 115–119.
- (20) PATTY: Beurskens, P. T.; Admiraal, G.; Beurskens, G.; Bosman, W. P.; Garcia-Granda, S.; Gould, R. O.; Smits, J. M. M.; Smykalla, C. *The DIRDIF program system*; Technical Report of the Crystallography Laboratory, University of Nijmegen: Nijmegen, The Netherlands, 1992.
- (21) DIRDIF99: Beurskens, P. T.; Admiraal, G.; Beurskens, G.; Bosman, W. P.; de Gelder, R.; Israel, R.; Smits, J. M. M. *The DIRDIF-99 program system*; Technical Report of the Crystallography Laboratory, University of Nijmegen: Nijmegen, The Netherlands, 1999.
- (22) CRYSTALS: Watkin, D. J.; Prout, C. K.; Carruthers, J. R.; Betteridge, P. W. *CRYSTALS. Issue 10*; Chemical Crystallography Laboratory: Oxford, England, 2000.